Biochemical and Biophysical Research Communications 434 (2013) 572–576

Contents lists available at SciVerse ScienceDirect

Biochemical and Biophysical Research Communications

journal homepage: www.elsevier.com/locate/ybbrc

Global cerebral ischemia induces increased expression of multiple retrotransposons

Shu Wang, Stephen Kelly *

Brain Injury and Repair Laboratory, New Jersey Neuroscience Institute, Edison, NJ, USA

ARTICLE INFO

Article history:
Received 25 March 2013
Available online 11 April 2013

Keywords:
Cerebral ischemia
Retrotransposons
Intracisternal A-particle (IAP)
Long interspersed nucleotide element 1 (L1)
DNA methylation

ABSTRACT

Retrotransposons (RTs) account for ~45% of the mammalian genome. They are capable of inserting into new genomic locations, which can result in deleterious outcomes. We examined the response of nine RTs to global cerebral ischemia (GCI) and explored the DNA methylation status of the two significantly altered RTs. Seven of the nine RTs were significantly increased at 24 h post-insult in ischemic hippocampus. GCI also led to a significant decrease in the DNA methylation status of intracisternal A-particle (IAP) RT, but had no marked effect upon DNA methylation of long interspersed nucleotide element 1 (L1) RT. In summary, GCI produced marked increases in RT RNA expression and had a differential effect on the DNA methylation status of two RTs in vulnerable hippocampal neurons destined to die. These data suggest that RTs may play an active role in ischemic brain pathology and that these endogenous mutagens and their regulatory elements could be targeted as potential therapeutic targets in this devastating condition.

1. Introduction

Approximately 45% of the mammalian genome is comprised of transposable elements, which can be divided into two major classes: DNA transposons and retrotransposons (RTs) [1,2]. Of the two, RTs are significantly more common and are transcribed into RNA, which is reverse-transcribed into double stranded DNA capable of inserting itself into new locations within the genome [3]. This can lead to insertional mutations in protein-coding genes, which can affect their expression by regulatory elements including promoters, splice donors/acceptors and polyadenylation signals from RTs [4]. It was also found that the insertion of retrotransposons can induce heterochromatin formation and expansion, thereby silencing neighbor genes [5]. In some instances, RT insertion can directly lead to genetic disorders [6,7]. As well as contributing to genetic disorders expression of autonomous L1 has been shown to create double strand breaks (DSBs) in genomic DNA, which lead to apoptosis in cancer cells [8,9]. While, direct inhibition of L1 RT significantly reduced ischemic heart damage [10]. Moreover, VL30 retrotransposition has been linked with a caspase-independent and p53-dependent death pathway, which is associated with mitochondrial and lysosomal damage [11].

Retrotransposons are believed to be maintained in a transcriptionally inactive state by DNA methylation [12]. A number of key factors are now know to regulate *de novo* DNA methylation, including, DNA methylases, Piwi-like genes and their interacting RNAs (piRNAs) [13–18]. Until recently it was believed that RTs were not active in somatic tissues due to the naturally elevated state of DNA methylation in their regulatory DNA sequences. Accumulating evidence however indicates that RTs could be activated in somatic tissues in normal or pathological conditions. Both short interspersed nucleotide element-2 (SINE B2) and virus like 30S element (VL30) expression has been reported in adult rodent brain [19,20], while intracisternal A-particles (IAP) have been observed in adult neurons and found to be inserted in a number of genes within the brain [21–28]. The long interspersed nucleotide element-1 (L1) is also now known to be expressed in human and mouse brain tissues including hippocampus and to contribute to somatic mosaicism in neuronal precursor cells [29,30].

In the current study, we examined the RNA levels of nine RTs in the selectively vulnerable hippocampus in response to GCI and explored the effects of DNA methylation status upon two upregulated RTs, IAP and L1.

2. Methods

2.1. GCI

The Seton Hall University IACUC committee approved all animal experiments. Mice were obtained from a commercial vendor (Taconic Farms Inc.) and were housed in compliance with AAALAC guidelines. GCI was induced in adult, male C57BL/6 mice ($n = 35$, 20–25 g) by bilateral common carotid artery occlusion (BCCAo) as described previously [31,32]. In brief, mice were assigned randomly to sham-operated or 20 min BCCAo groups. In all mice, surgical anesthesia was induced with isoflurane (5%) in medical air and maintained throughout the procedure at 1–2% via a facemask.

* Corresponding author. Address: New Jersey Neuroscience Institute, JFK Medical Center, Edison, NJ 08818, USA. Fax: +1 732 767 2902.
E-mail address: ischemia@gmail.com (S. Kelly).

0006-291X/$ - see front matter © 2013 Elsevier Inc. All rights reserved.
http://dx.doi.org/10.1016/j.bbrc.2013.03.116

A small ventral neck incision was used to expose the common carotid arteries and place surgical silks (3–0) around them. To induce GCI, the arteries were occluded by applying tension to the surgical silks and placing aneurysm clips (50–80 g closing pressure) on each vessel. Clips were removed after 20 min, carotid patency observed, the neck sutured and anesthesia discontinued. Sham-operated mice were treated identically, except that the carotids were not occluded. Cerebral blood flow (CBF) in the left and right forebrain was monitored before, during and after BCCAo using a Perimed PeriFlux system 5000 laser Doppler system equipped with two 418 probes. Only mice with a reduction in CBF of 75% or more in both left and right hemispheres were employed in this study. Rectal temperature was maintained at 37 ± 0.5 °C throughout. At the end of the procedure, each mouse was injected subcutaneously with sterile saline (0.5 ml), placed in its home cage on a heating mat for 30 min post-operatively and returned to a temperature-controlled room.

2.2. Assessing ischemic neuronal damage

Sham-operated and GCI mice ($n = 8$) were terminally anesthetized at 24 or 72 h post-surgery and perfused transcardially with paraformaldehyde (4%) as described previously [31]. Decapitated heads were stored overnight in paraformaldehyde. The following day, the brains were removed, cut into three coronal blocks (3 mm thick), processed and embedded in paraffin wax. Seven-micron thin sections were prepared on a microtome and stained with hematoxylin and eosin. Brightfield microscopy was used to identify healthy and ischemic neurons.

2.3. RNA extraction

Mice were anesthetized at one, six and 24 h post-surgery, decapitated and their brains removed. Individual hippocampi were rapidly dissected and immediately stored in RNA later solution. Total RNA was isolated from each individual hippocampus using a mirVANA miRNA isolation kit (Ambion), and the concentration was measured by QubitTM RNA assay kit (Invitrogen). Integrity/quality was analyzed on a denaturing 15% polyacrylamide gel as described in the manufacturer's instructions.

2.4. qRT-PCR (quantitative polymerase chain reaction with reverse transcription)

Total RNA was treated with Turbo Dnase (Ambion) according to the manufacturer's instructions. The Dnase treated total RNA was reverse transcribed using Superscript III reverse transcriptase (Invitrogen) with random hexamers. The cDNA was diluted and qPCR was carried out using Sybr green master mix (Applied Biosystems) on a StepOne real-time PCR sytem (Applied Biosystems). GAPDH was used to normalize the expression of all RTs, TIGGER and MULV. Primer sequences used are provided in Table 1.

2.5. DNA methylation assays

DNA was extracted from our samples and the concentration measured by Qubit® dsRNA BR assay kits (Invitrogen). DNA was treated with sodium bisulfate using EpiTect kit (Qiagen). The LTR region of IAP on chromosome 3qD was arbitrarily selected for analysis by nested PCR using primers IAP Ch3-bisF1 and IAP-bisR1, IAP-bisF2 and IAP-bisR2 [17]. The 5′UTR-region of L1 (type A) was amplified using primers of methylL1-F and methylL1-R [16]. Primer sequences used are provided in Table 1. The PCR products of L1A and IAP were cloned into pGEM-easy vector (Promega), and twenty-four clones picked at random were sequenced. DNA methylation status was analyzed using BIQ Analyzer software.

Table 1
Primers used for RT-PCR and bisulfite sequencing.

	Sequence (5′–3′)
RT-PCR	
ETN – *f*	CAGGCTTTGGAGACAATAGGG
ETN – *r*	TCTCTCAGGGAACTCAGAAACG
IAP – *f*	CCTTTGTTGCCCAGGTAAGTC
IAP – *r*	CACTGTAGCCAGTTGTGACCAG
GAPDH – *f*	ACTCCCACTCTTCCACCTTCGATGCCG
GAPDH – *r*	ATGTAGGCCATGAGGTCCACCACCCTG
MERVL – *f*	CCCATCATGAGCTGGGTACT
MERVL – *r*	CGTGCAGATCCATCAGTAAA
GUSB – *f*	ATAAGACGCATCAGAAGCCG
GUSB – *r*	ACTCCTCACTGAACATGCGA
MT – *f*	ATGTCTTGGGGAGGACTGTG
MT – *r*	AGCCCCAGCTAACCAGAACT
MULV – *f*	GGCGCCCCGTACAAGATTTCATA
MULV – *r*	GATAACGGGCCTGCCTTCACCTC
ORF 2B – *f*	CTGGCGAGGATGTGGAGAA
ORF 2B – *r*	CCTGCAATCCCAACAAT
ORR1 – *f*	CTTTAGTTGATGGCCCAGGA
ORR1 – *r*	CCAACTCTGCCCTCTGTAGC
SINE B1 – *f*	GTGGCGCACGCCTTTAATC
SINE B1 – *r*	GACAGGGTTTCTCTGTGTAG
SINE B2 – *f*	GAGATGGCTCAGTGGTTAAG
SINE B2 – *r*	CTGTCTTCAGACACTCCAG
TIGGER – *f*	GTGTCAGGAGGTTTCAAAGGCTC
TIGGER – *r*	CGCTCTCTTGAAGGCAAGGACTC
VL30 – *f*	CCTTTGTTGCCCAGGTAAGTC
VL30 – *r*	CACTGTAGCCAGTTGTGACCAG
Bisulfite	
IAP bis - *f1*	GTTTGTAATGGTGGGAGA
IAP-bis - *r1*	AAATAAAATATCCCTCC
IAP-bis - *f2*	TTGTGTTTTAAGTGGTAAATAAATAATTTG
IAP-bis - *r2*	CAAAAAAAACACACAAACCAAAAT
MethylL1 – *f*	AAGTTATAAATAATTTTTTGGGGTT
MethylL1 – *r*	AAACAAACACTATAATCCACTCACC

3. Results

3.1. GCI pathology

GCI leads to delayed neuronal death in selectively vulnerable brain regions. In our BCCAo model, a small subset of neurons within the highly vulnerable CA1 hippocampal field exhibited signs of ischemic cell change by 24 h post-insult (Fig. 1). In mice allowed to survive for 72 h post-GCI, extensive neuronal loss in CA1 is observed (Fig. 1). The data reported in this study were collected at 1, 6 and 24 h post GCI in order to assess ischemia-induced changes in cells destined to die, rather than in cells that have already died.

3.2. RT expression following GCI

qRT-PCR showed that seven RTs (IAP, L1, MT, ORR1, SINE B1, SINE B2 and VL30) were significantly upregulated in ischemic hippocampus at 24 h post-insult and two were not significantly different (ETN and MERVL Fig. 2). The three most markedly increased RTs at 24 h (IAP, SINE B2 and VL30) were also measured at 1 and 6 h after GCI to establish the time course of this response. Significant increases were observed at these earlier time points compared with shams, but these were dwarfed by the increases observed at 24 h. In addition to RTs, we also found that GCI upregulated the expression of the TIGGER DNA transposon and a retrovirus MuLV (Fig. 2).

3.3. DNA methylation of IAP but not L1 was significantly reduced by ischemic insult

To examine the contribution of DNA methylation to IAP and L1 upregulation, we performed bisulfate sequencing. The results

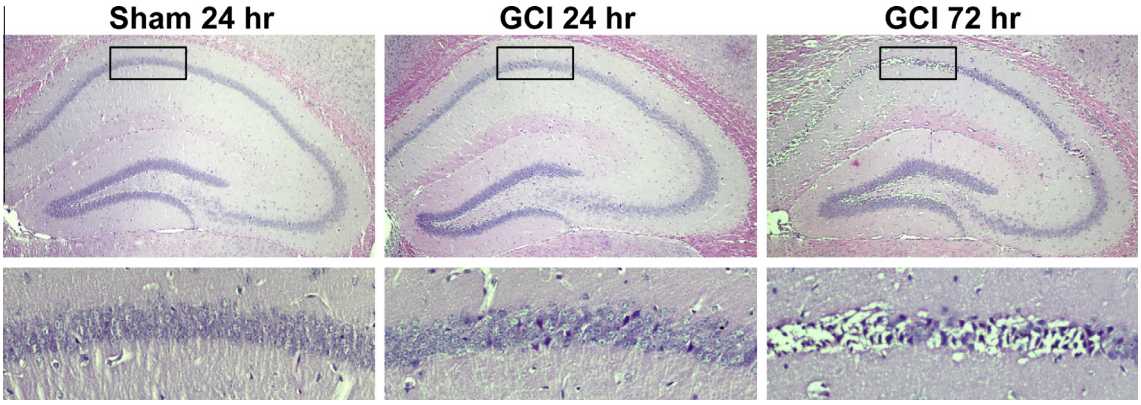

Fig. 1. No signs of substantial hippocampal neuronal death at 24 h post-GCI. Representative examples of hematoxylin and eosin stained brain sections from sham and GCI mice taken at 24 h post-surgery, and GCI mice taken at 72 h post-surgery. Upper panels show low power images of dorsal hippocampus, lower panels show higher power images of neurons in the highly-susceptible CA1 subfield (boxes). Sham 24 h section (left panels) shows no signs of ischemic damage. GCI 24 h section (middle panels) shows some signs of ischemic damage in a handful of neurons that appear darker and somewhat shrunken. In contrast, the GCI 72 h section (right panels) shows extensive ischemic damage in the form of many dark, shrunken, pyknotic nuclei with associated eosinophylic cytoplasm and large gaps in the neuropil surrounding these cells.

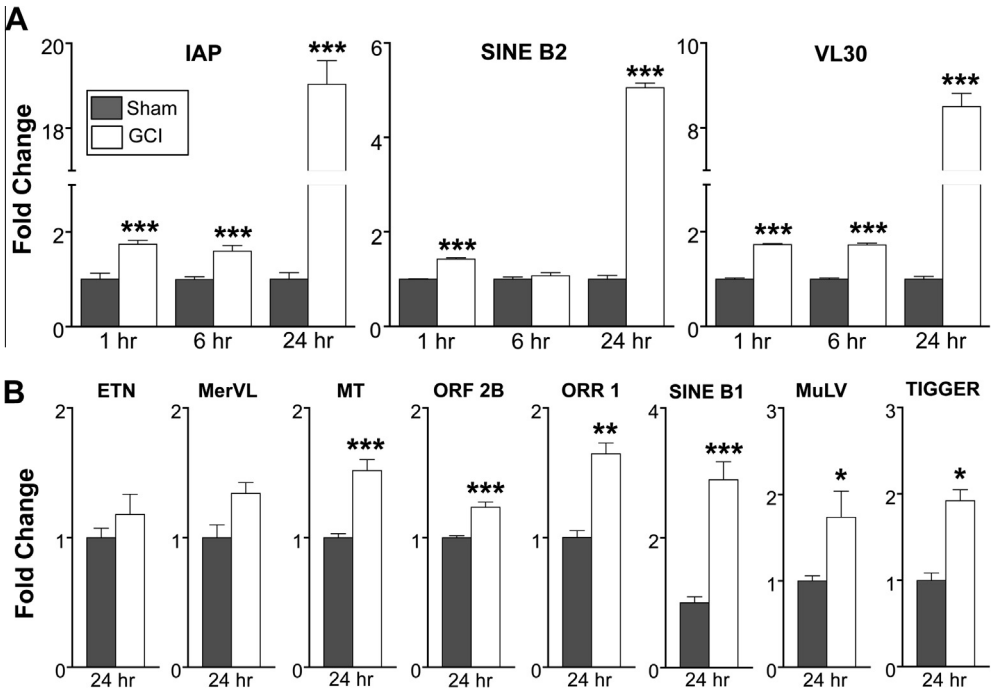

Fig. 2. GCI increases RT expression in hippocampus. GCI increases expression of seven of nine RTs, TIGGER DNA transposon and MULV retrovirus in hippocampus at 24 h post-insult (A and B). The three most markedly increased RTs IAP, SINE B2 and VL30 were also examined at 1 and 6 h post-GCI (A). While all three were increased significantly at both time points, there was a dramatic increase in expression observed between 6 h and 24 h post-GCI. qRT-PCR was performed in triplicate and data are expressed as mean fold change plus or minus standard deviation, unpaired Student's *t*-test was used to compare means. ($^{***}p < 0.0001$, $^{**}p < 0.001$, $^{*}p < 0.05$).

indicated that the DNA methylation status of CpG islands in the 5′LTR of IAP was significantly reduced by ischemic insult (38.2% versus 65% Fig. 3A). However, the DNA methylation status of the L1 regulatory sequence in hippocampus following GCI was only marginally lower than that in sham-operated mice at 89.3% versus 92%, respectively (Fig. 3B).

4. Discussion

The present study shows that GCI induces marked increases in the expression of a number of RTs in the vulnerable hippocampal region. These findings complement and extend upon two earlier studies in rat GCI and FCI models. We show that SINE B2 in increased in a mouse model of GCI, which correlates with the finding of Kalkkila et al. [19] who reported this in a rat model of GCI. We also show that GCI in mouse increases the expression of VL30, which was previously shown to increase in rat hippocampus following FCI [20]. Several other RTs that had not been studied in ischemic brain were also significantly increased. Chief among these was the defective endogenous retrovirus-like mobile element, IAP, which was dramatically upregulated (~19-fold) following GCI. We also show that IAP and L1 may be differentially influenced by DNA methylation status following GCI.

While the precise role of RTs in the brain and other somatic cell types remains unclear, they have been linked with genetic disorders [6,7], impaired cellular function and cell death [8,9,11]. L1 RT, which is one of the more studied RTs and is known to be active in mouse and human brain, has been shown to play roles in brain cell diversity, the physiologic consequences of neuronal plasticity and Rett syndrome in recent years [29,30,33–35]. Luchinetti et al.

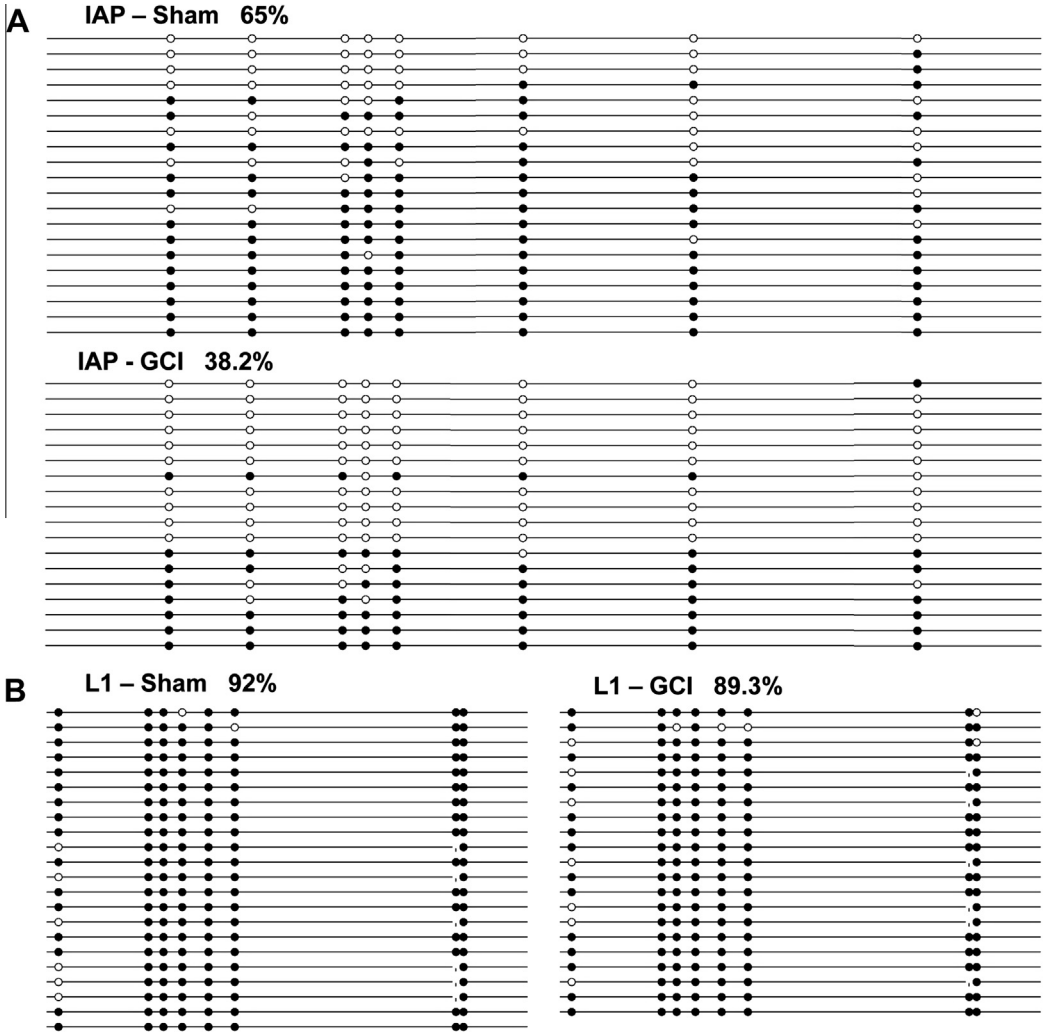

Fig. 3. GCI significantly reduces DNA methylation status of IAP. Lollipop representation of the IAP (A) and L1 (B) sequences obtained after bisulfate treatment of sham- and GCI operated hippocampal DNA. Black circles correspond to methylated Cs, white circles correspond to unmethylated Cs, and small vertical lines without a circle correspond to missing values (e.g. caused by allelic polymorphisms).

[10] also showed that L1 expression was increased in ischemic heart and that direct inhibition of L1 using antisense nucleotides markedly improved cardiac function while reducing infarct size. These findings and our observation that RT expression is widely increased in vulnerable neurons destined to die following GCI strongly suggest that RTs may play an active pathologic role in ischemic brain injury. IAP was the most significantly increased RT in our study and could represent a novel factor contributing to ischemic brain pathology. As well as being implicated in various cancers, IAP has been shown to be expressed neurons and brain [21–28,33–35]. Moreover, IAP insertions have also been shown to affect the properties of a number of genes in brain, many of which can be directly linked with ischemic brain injury [19,20]. One such example of this is human ADAMTS13 where IAP insertions have lead to generation of variant proteins that were less effective at cleaving von Willenbrand factor [36].

IAP loci are highly methylated and silenced in mouse somatic cells [37,38]. We found that GCI led to a marked decrease in the DNA methylation status of CpG islands in IAP regulatory sequence (38.2% versus 65%), suggesting that this may be, at least in part, responsible for the dramatic increase in IAP expression observed in our study. In contrast, the DNA methylation status of CpG islands in L1 regulatory sequences was not significantly altered by GCI (89.3% versus 92%) suggesting that the observed increases in L1 expression may be due to other mechanisms, such as Piwi-like genes or piRNA.

In the present study we have shown that GCI leads to significantly increased expression of RTs in a cell population destined to die, suggesting a role for these endogenous mutagens in ischemic brain pathology. Furthermore, by investigating the DNA methylation status of two upregulated RTs, IAP and L1, we found that RTs may be regulated differentially following GCI. We were particularly intrigued by the dramatic increase observed in IAP expression following GCI and by the fact that this increase appears to be, at least in part, regulated by a reduced DNA methylation. We have commenced further studies to explore the role of IAP in ischemic brain injury. It is our opinion that RTs could be valid targets for neuroprotective strategies to treat ischemic brain injury and that DNA methylation, Piwi-proteins and piRNAs represent excellent, novel candidates that could be harnessed to achieve this.

Acknowledgment

We thank Ms. Joanne Chien for technical assistance.

References

[1] E.S. Lander, L.M. Linton, B. Birren, Initial sequencing and analysis of the human genome, Nature 409 (2001) 860–921.

[2] R. Cordaux, M.A. Batzer, The impact of retrotransposons on human genome evolution, Nat. Rev. Gen. 10 (2009) 691–703.
[3] P. Liang, W. Tang, Database documentation of retrotransposon insertion polymorphisms, Front Biosci. 4 (2012) 1542–1555.
[4] D.C. Hancks, H.H. Kazazian Jr., Active human retrotransposons: variation and disease, Curr. Opin. Genet. Dev. 22 (2012) 191–203.
[5] R. Rebollo, M.M. Karimi, M. Bilenky, et al., Retrotransposon-induced heterochromatin spreading in the mouse revealed by insertional polymorphisms, PLoS Genet. 7 (2011) e1002301.
[6] J.M. Chen, P.D. Stenson, D.N. Cooper, C. Ferec, A systematic analysis of LINE-1 endonuclease dependent retrotranspositional events causing human genetic disease, Hum. Genet. 117 (2005) 411–427.
[7] P.A. Callinan, M.A. Batzer, Retrotransposable elements and human disease, Genome Dyn. 1 (2006) 104–115.
[8] S.L. Gasior, T.P. Wakeman, B. Xu, P.L. Deininger, The human LINE-1 retrotransposon creates DNA double-strand breaks, J. Mol. Biol. 357 (2006) 1383–1393.
[9] S.M. Belgnaoui, R.G. Gosden, O.J. Semmes, A. Haoudi, Human LINE-1 retrotransposon induces DNA damage and apoptosis in cancer cells, Cancer Cell Int. 6 (2006) 13.
[10] E. Lucchinetti, J. Feng, R. Silva, et al., Inhibition of LINE-1 expression in the heart decreases ischemic damage by activation of Akt/PKB signaling, Physiol. Genomics 25 (2006) 314–324.
[11] D. Noutsopoulos, G. Markopoulos, G. Vartholomatos, et al., VL30 retrotransposition signals activation of a caspase-independent and p53-dependent death pathway associated with mitochondrial and lysosomal damage, Cell Res. 20 (2010) 553–562.
[12] C.P. Walsh, J.R. Chaillet, T.H. Bestor, Transcription of IAP endogenous retroviruses is constrained by cytosine methylation, Nat. Genet. 20 (1998) 116–117.
[13] D. Bourc'his, T.H. Bestor, Meiotic catastrophe and retrotransposon reactivation in male germ cells lacking Dnmt3L, Nature 431 (2004) 96–99.
[14] K. Hata, M. Kusumi, T. Yokomine, E. Li, H. Sasaki, Meiotic and epigenetic aberrations in Dnmt3L-deficient male germ cells, Mol. Reprod. Dev. 73 (2006) 116–122.
[15] Y. Kato, M. Kaneda, K. Hata, et al., Role of the Dnmt3 family in *de novo* methylation of imprinted and repetitive sequences during male germ cell development in the mouse, Hum. Mol. Genet. 16 (2007) 2272–2280.
[16] M.A. Carmell, A. Girard, H.J. van de Kant, et al., MIWI2 is essential for spermatogenesis and repression of transposons in the mouse male germline, Dev. Cell 12 (2007) 503–514.
[17] S. Kuramochi-Miyagawa, T. Watanabe, K. Gotoh, et al., DNA methylation of retrotransposon genes is regulated by Piwi family members MILI and MIWI2 in murine fetal testes, Genes Dev. 22 (2008) 908–917.
[18] S. De Fazio, N. Bartonicek, M. Di Giacomo, et al., The endonuclease activity of Mili fuels piRNA amplification that silences LINE1 elements, Nature 480 (2011) 259–263.
[19] J.P. Kalkkila, F.R. Sharp, I. Kärkkäinen, et al., Cloning and expression of short interspersed elements B1 and B2 in ischemic brain, Eur. J. Neurosci. 19 (2004) 1199–1206.
[20] W.J. Costain, I. Rasquinha, T. Graber, et al., Cerebral ischemia induces neuronal expression of novel VL30 mouse retrotransposons bound to polyribosomes, Brain Res. 1094 (2006) 24–37.
[21] R. Peach, W.E. Koch, A cytoplasmic inclusion in mouse trigeminal neurons, Am. J. Anat. 140 (1974) 439–444.
[22] J.W. Gaubatz, B. Arcement, R.G. Cutler, Gene expression of an endogenous retrovirus-like element during murine development and aging, Mech. Aging Dev. 57 (1991) 71–85.
[23] M.L. Ware, J.W. Fox, J.L. González, et al., Aberrant splicing of a mouse disabled homolog, mdab1, in the scrambler mouse, Neuron 19 (1997) 239–249.
[24] S.M. Wilson, B. Bhattacharyya, R.A. Rachel, et al., Synaptic defects in ataxia mice result from a mutation in Usp14, encoding a ubiquitin-specific protease, Nat. Genet. 32 (2002) 420–425.
[25] H. Sugino, T. Toyama, Y. Taguchi, et al., Negative and positive effects of an IAP-LTR on nearby Pcdaalpha gene expression in the central nervous system and neuroblastoma cell lines, Gene 337 (2004) 91–103.
[26] J. Xiao, M.S. Ledoux, Caytaxin deficiency causes generalized dystonia in rats, Brain Res. Mol. Brain Res. 141 (2005) 181–192.
[27] X.Y. Sun, Z.Y. Chen, Y. Hayashi, et al., Insertion of an intracisternal A particle retrotransposon element in plasma membrane calcium ATPase 2 gene attenuates its expression and produces an ataxic phenotype in joggle mutant mice, Gene 411 (2008) 94–102.
[28] R.G. Hunter, G. Murakami, S. Dewell, et al., Acute stress and hippocampal histone H3 lysine 9 trimethylation, a retrotransposon silencing response, Proc. Natl. Acad. Sci. USA 109 (2012) 17657–17662.
[29] N.G. Coufal, J.L. Garcia-Perez, G.E. Peng, et al., L1 retrotransposition in human neural progenitor cells, Nature 460 (2009) 1127–1131.
[30] A.R. Muotri, V.T. Chu, M.C. Marchetto, et al., Somatic mosaicism in neuronal precursor cells mediated by L1 retrotransposition, Nature 435 (2005) 903–910.
[31] S. Kelly, J. McCulloch, K. Horsburgh, Minimal ischaemic neuronal damage and HSP70 expression in MF1 strain mice following bilateral common carotid artery occlusion, Brain Res. 914 (2001) 185–195.
[32] S. Kelly, A. Bieneman, K. Horsburgh, et al., Targeting expression of hsp70i to discrete neuronal populations using the Lmo-1 promoter: assessment of the neuroprotective effects of hsp70i *in vivo* and *in vitro*, J. Cereb. Blood Flow Metab. 21 (2001) 972–981.
[33] A.R. Muotri, M.C. Marchetto, N.G. Coufal, et al., L1 retrotransposition in neurons is modulated by MeCP2, Nature 468 (2010) 443–446.
[34] A.R. Muotri, C. Zhao, M.C. Marchetto, F.H. Gage, Environmental influence on L1 retrotransposons in the adult hippocampus, Hippocampus 19 (2009) 1002–1007.
[35] C.A. Thomas, A.C. Paquola, A.R. Muotri, LINE-1 retrotransposition in the nervous system, Annu. Rev. Cell Dev. Biol. 28 (2012) 555–573.
[36] W. Zhou, E.E. Bouhassira, H.M. Tsai, An IAP retrotransposon in the mouse ADAMTS13 gene creates ADAMTS13 variant proteins that are less effective in cleaving von Willebrand factor multimers, Blood 110 (2007) 886–893.
[37] L.K. Hutnick, X. Huang, T. Loo, et al., Repression of Retrotransposal Elements in Mouse Embryonic Stem Cells Is Primarily Mediated by a DNA Methylation-independent Mechanism, J. Biol. Chem. 285 (2010) 21082–21091.
[38] F. Gaudet, W.M. Rideout, A. Meissner, et al., Dnmt1 expression in pre- and postimplantation embryogenesis and the maintenance of IAP silencing, Mol. Cell Biol. 24 (2004) 1640–1648.